

11-2-2010

Hydrogen Absorption Induced Slow Crack Growth in Austenitic Stainless Steels for Petrochemical Pressure Vessel Industries

Ronnie Higuchi Rusli

Graduate Program of Engineering, University of Indonesia, Jakarta 10430, Indonesia Visiting Research Scientist at Sumitomo Steel Industries Ltd., Research & Development Center, Japan,
ronnie_rusli@yahoo.com

Follow this and additional works at: <https://scholarhub.ui.ac.id/mjt>



Part of the [Chemical Engineering Commons](#), [Civil Engineering Commons](#), [Computer Engineering Commons](#), [Electrical and Electronics Commons](#), [Metallurgy Commons](#), [Ocean Engineering Commons](#), and the [Structural Engineering Commons](#)

Recommended Citation

Rusli, Ronnie Higuchi (2010) "Hydrogen Absorption Induced Slow Crack Growth in Austenitic Stainless Steels for Petrochemical Pressure Vessel Industries," *Makara Journal of Technology*: Vol. 14 : No. 2 , Article 10.

DOI: 10.7454/mst.v14i2.702

Available at: <https://scholarhub.ui.ac.id/mjt/vol14/iss2/10>

This Article is brought to you for free and open access by the Universitas Indonesia at UI Scholars Hub. It has been accepted for inclusion in Makara Journal of Technology by an authorized editor of UI Scholars Hub.

HYDROGEN ABSORPTION INDUCED SLOW CRACK GROWTH IN AUSTENITIC STAINLESS STEELS FOR PETROCHEMICAL PRESSURE VESSEL INDUSTRIES

Ronnie Higuchi Rusli

Graduate Program of Engineering, University of Indonesia, Jakarta 10430, Indonesia
Visiting Research Scientist at Sumitomo Steel Industries Ltd., Research & Development Center, Japan

E-mail: ronnie_rusli@yahoo.com

Abstract

Type 304L and type 309 austenitic stainless steels were tested either by exposed to gaseous hydrogen or undergoing polarized cathodic charging. Slow crack growth by straining was observed in type 304L, and the formation of α' martensite was indicated to be precursor for such cracking. Gross plastic deformation was observed at the tip of the notch, and a single crack grew slowly from this region in a direction approximately perpendicular to the tensile axis. Martensite formation is not a necessary condition for hydrogen embrittlement in the austenitic phase.

Keywords: austenitic stainless steels, fracture, hydrogen embrittlement, martensitic, pressure vessels

1. Introduction

Stainless steels weld overlaid cladding pressure vessels (PV) is a necessary procedure and increasingly needed for PV in the prochemical industries. PV must be capable of being used in extreme environments for processing heavy crude oil in which hydrogen up take can be introduced into the cladding metal surface. Because of their importance as corrosion-resistant materials, the behavior of austenitic stainless steels in such harsh environments has attracted considerable attention. This work has demonstrated that significant ductility losses occurred when the material is tested dynamically after being internally charged with hydrogen [1-7] or while being exposed to a gaseous hydrogen environment [8-13]. Delayed failures by hydrogen absorption have been reported under static stresses, and one of the objectives of the present work was to investigate the possibility hydrogen absorption induced slow crack growth.

A further objective was to clarify the role of austenite stability, i. e., its tendency to transform to α' and ϵ martensites, on the embrittlement process. This subject has become controversial [6-9,14-17], due in part to comparison of data obtained from alloys which were not well characterized. For example, it cannot be assumed that a nominally stable steel will always consistently be stable, or, conversely, that a nominally unstable grade will always under go strain-induced martensitic transformation, or that a steel which is stable under one

type of deformation will be stable under a different mode. Furthermore, the possible effect of absorbed hydrogen on austenite stability cannot be overlooked. In the present work, these uncertainties were analyzed experimentally to determine the presence or absence of α' martensite before and after testing in the hydrogen-bearing environments.

2. Experiment

The studies were carried out with a sensitized type 304L and a stable type 309 austenitic stainless steels with composition shown in the Table 1. These stainless steels were selected because the gamma phase in the former could be expected to transform to α' (and/or ϵ) as a result of cooling or stressing, whereas the gamma phase in the latter was anticipated to be highly stable. These steels were to commercial grade, and were received in the form of sheet, 1.6 mm thick. Tensile specimens of dimensions 12 cm x 1.6 mm were cut from the sheet with their long axes parallel to the rolling direction, and annealed for 2,5h at 1050 °C in argon, purged and quenched into water at room temperature. Examination with a ferrite detector indicated that no detectable α' martensite was present at room temperature. After heat treatment, all samples were electropolished in a solution of 65 vol. Pct. Orthophosphoric acid and 35 vol. Pct. Sulfuric acid at 10-12 V for 20 min. Prior to testing, a saw cut, ~3 mm deep, was made at one edge of each specimen.

Table 1. Chemical Composition of Alloys, in wt %

Type of Stainless Steels	Chemical Composition							
	Cr	Ni	Mn	C	Mo	N	Si	Ti
304L	18.39	8.61	1.40	1.60	0.10	-	0.42	0.09
309	23.47	15.47	1.62	0.05	0.22	0.015	0.50	-

The single edge notched specimens were tested under constant load using a MTS electrohydraulic closed-loop system. The test were carried out while the specimens were either under a gaseous hydrogen atmosphere or while the specimens were undergoing cathodic polarization. The tests in hydrogen gas were carried out by enclosing the notched region in a glass chamber and maintaining a flow of dry, high purity hydrogen (Linde Ultra-High Purity Grade) under a positive pressure of ~ 7 kPa cathodic-polarization tests were carried out at room temperature in a 1.5 N sulfuric acid solution containing 250 mg of sodium arsenite per liter using a platinum anode and a current density of 40 mA/cm².

In each case, the initiation and propagation stages of cracking were observed by means of an optical stereo microscope and simultaneously recorded. After failure, the fracture surfaces were examined with a scanning and field emission transmission electron microscopes (SEM and FE-TEM). A measure of the amount of α' martensite present at the fracture surfaces was obtained using a commercial ferrite detector, capable of detecting as little as 0.095 vol. Pct of α' martensite. This instrument, which in effect measures magnetic permeability, has a probe with two hemispherical poles of radius 1.25 mm, spaced 4.0 mm apart, and these were placed in contact with the fracture surfaces and, in other measurements, with the side faces of the specimens. The ferrite detector was also used to determine the M_D temperature, defined as the highest temperature at which straining the notched specimens to rupture produced detectable martensite. The M_D of the type 304L alloy was found to be ~ 110 °C; no α' martensite was detected in the type 309 specimens under any condition.

Both specimens for SEM and TEM observation were prepared by electro-chemical polishing using a twinjet-polishing method. The Electrolytic solution was mixture of perchloric acid, methanol, and 2-n-butoxyethanol (blend ratio of 1 : 10 : 6). The foil specimens were polished at 25 V and 243 K for SEM and FE-TEM experiments.

3. Results and Discussion

Stainless steel type 304L specimens tested in gaseous hydrogen. Preliminary tests in air at room temperature established that the notched specimens fractures by ductile shear at a nominal stress (e.i., based on the

original cross-sectional area at the notch) of 390 MPa loading in air for extended on subsequent testing. Using the ferrite detector, the amount of α' martensite at the ductile fracture surfaces was found to be $2.0 \pm 0.6\%$. As in subsequent cases, this figures represents the average of at least six determinations taken at various positions on the fracture surface.

Constant-load tests in hydrogen at room temperature indicated that slow crack growth occurred when the nominal stresses exceeded approximately 320 MPa. These tests were carried out by incrementally increasing the loads until propagation occurred; incubation times of up to 3h were observed. Gross plastic deformation was observed at the tip of the notch, and a single crack grew slowly from this region in a direction approximately perpendicular to the tensile axis. Rapid overload failure occurred when the crack length attained about 1/3 of the width of the specimen. The average velocity of slow crack growth found to be ~ 2.3 $\mu\text{m/s}$.

The fracture surfaces produced by slow crack growth were flat and approximately perpendicular to the stress axis. Examination with the SEM (see Fig. 2c) indicated that these surfaces were transgranular and cleavage-like as reported elsewhere, TEM result shown in Fig. 1 in bright field images, shows carbides precipitated near the grain boundary surfaces produced by overload failure were inclined at 45° to the tensile axis and were characteristic of ductile rupture. i.e., they exhibited the "dimpled" structure produced by void nucleation and coalescence from carbide particels. The magnetic technique indicated the presence of 4.0 ± 0.5 pct. α' at the fracture surface produced by slow crack growth, and 1.4 ± 0.6 pct. α' at the ductile fracture surface. Measurements on the side faces indicated that the martensitic phase was confined to a region extending approximately 2-3 nm on each side of the crack (see Fig 2a and 2b).

Tests in gaseous hydrogen were also carried out at 150 °C, that is well above the M_D temperature. The result shows no slow crack growth was observed even at constant stresses close to the ultimate. Fracture surfaces produced by tensile overload were completely ductile in appearance, and magnetic testing detected no α' at these fracture surfaces.

Stainless steel type 304L specimens tested while cathodically polarized. These tests, carried out in the 1.5 N sulfuric acid electrolyte at room temperature, produced slow crack growth when the specimens were subjected to constant stresses exceeding about 250 MPa. The average velocity of these cracks was ~ 2.6 $\mu\text{m/s}$. Again, rapid ductile rupture occurred as the final fracture mode, and the morphology of the fracture surfaces was similar to that of specimens tested in gaseous hydrogen in that numerous cracks were

initiated. Thus, during cathodic polarization, a large number of cracks were observed in the region of the notch, and many secondary cracks were observed on the side faces adjacent to the main fracture. The crystallographic nature of the secondary cracks was apparent from the abrupt changes in direction when they intersected twin or grain boundaries (Fig. 3a). The amount of α' martensite detected at the cleavage-like fracture surfaces was 4.1 ± 0.6 pct. Again, the martensitic phase was confined to a small region adjacent to the fracture face. Cathodic polarization in the absence of stress did not produce any transgranular cracking, but extended charging 2-3 days resulted in some intergranular attack. No α' martensite was detected in these specimens.

Stainless Steel Type 309 specimens tested in gaseous hydrogen. Constant-load tests in air gaseous hydrogen at room temperature failed to produce slow crack growth. Rapid overload fracture occurred when the specimens were subjected to nominal stresses exceeding ~ 380 MPa, and the magnetic technique revealed no evidence of α' martensite in the fractured specimens.

No slow crack growth was observed in specimens stressed while cathodically polarized in the 1 N sulfuric acid. However, at large nominal stresses (~ 350 MPa) numerous shallow cracks appeared on the side face in the region of the notch (Fig. 3b). In contrast to the case of type 304L (Fig. 2c) these cracks appeared less crystallographic and were approximately perpendicular

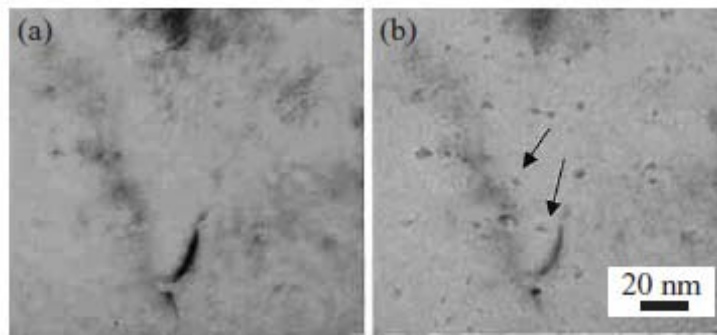


Figure 1. Bright Field FE-TEM (a) Image of Carbides Precipitated Near the Grain Boundary of Sensitized Stainless Steel Type 304L, (b) Focused Image Shows the Direction (Arrows) of Carbides Movement in the Slip Plane

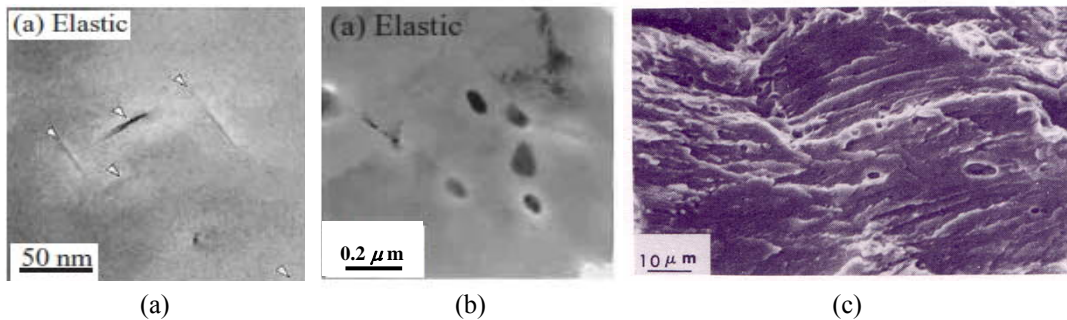


Figure 2. FE-TEM and SEM Images of Typical Transgranular Fracture Surface Produced by Slow Cracks Along the (a) Slip Plane and (b,c) Carbides Precipitated in Type 304L Steel Elastic Tested in Gaseous Hydrogen

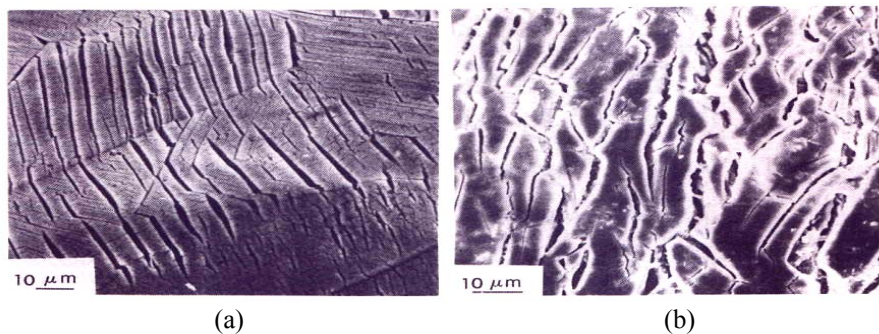


Figure 3. SEMs of Side Faces of Specimens Tested While Being Cathodically Charged, Showing Secondary Cracks in the Region of the Notch. (a) Type 304L, and (b) Type 309

to the direction of the stress axis. Failure of these specimens occurred following a considerable amount of necking, and the resulting fracture surface were ductile. No α' martensite was detected on the fracture surfaces. Prolonged charging (2-3 days) in the absence of stress produced some intergranular grooving and occasional transgranular cracks. There was no evidence for α' martensite in these specimens.

A significant feature of the results is the occurrence of slow crack growth in type 304L austenitic stainless in gaseous hydrogen, a phenomenon which does not appear to have not many reported previously. This form of embrittlement occurred at large stresses, namely ~70-80% of the fracture stress in air, and thus it might be argued that it is unlikely to be a concern in practice. However, the hydrogen fugacity was low in the present tests at 1 atmosphere pressure, and it is possible that more severe conditions will be encountered in the service, that might cause cracking at lower stresses. In the present studies for example, slow crack growth was observed at ~65% of the air fracture stress when the type-304L steel was stressed while being cathodically charged in the 1.5 N sulfuric acid solution. This may be significant to mention, that no slow crack growth was observed in the stable type 309 material [22].

This results also strongly suggest that the hydrogen-induced slow crack growth requires the formation of stress-induced α' martensite. Thus no slow crack growth alloy, and the specific role of the α' martensite has not been established, but several possibilities exist. The lattice diffusivity of hydrogen in the BCC form is $\sim 10^{-3}$ cm²/S and $\sim 10^{-12}$ cm²/s for the FCC phase [18-23], and therefore the martensite formed ahead of the advancing crack may simply provide a rapid-diffusion path for hydrogen atom to pass through. In this regard diffusivity of $\sim 5 \times 10^{-8}$ cm²/s, is fully compatible with transport in the α' but not in the γ phase.

A second possibility is that the α' martensite itself undergoes hydrogen embrittlement, and that the crack progresses through the martensite plates or through the α' to γ (gamma) interface. This possibility is consistent with the fact that the martensitic phase is known to be readily embrittled by hydrogen. On the other hand, the occurrence of limited brittle cracking in type 309 during cathodic polarization, Fig. 3b indicates that martensite formation is not a necessary condition for hydrogen embrittlement in the austenitic phase which is in agreement with the observations of other worker [24-25]. Thus on the basis of the present work, it is possible to distinguish whether the observed slow crack growth in type 304L involves hydrogen embrittlement of the stress-induced α' martensite, or of the austenite phase itself.

4. Conclusion

A further interesting feature of the present work is that the amount of martensite formation accompanying slow crack growth was greater than that for ductile rupture as suggested elsewhere, and that hydrogen entry may promote martensite formation. Work in progress on specimens precharged at high temperature has confirmed this effect, and thus we agree with other workers that the embrittlement of unstable stainless steel may be autocatalytic and martensite assisted hydrogen entry, and cracking occurred by martensite formation.

Acknowledgement

My Sincere thank due to Drs Y. Yamada, K. Yamazaki and T. Watanabe for their assistances and support of testing. This work as supported by the Japan Science & Engineering Foundation under grant number JSF DMR 07/4-24648.

References

- [1] J.D. Hobson, J. Hewitt, J. Iron. Steel Inst. 173 (1953) 131.
- [2] P. Blanchard, A.R. Troiano, Mem. Sci. Rev. Met. 57 (1960) 409.
- [3] Y.P. Nechay, K.V. Popov, Fiz. Met. Metallov. 14 (1962) 271.
- [4] M.B. Whiteman, A.R. Troiano, Corrosion 21 (1965) 53.
- [5] R. Lagneborg, J. Iron. Steel Inst. 207 (1969) 363.
- [6] M.L. Holzworth, Corrosion 25 (1969) 107.
- [7] L.K. Zamiryakin, Sov. Mater. Sci. 7 (1971) 9.
- [8] R.M. Vennett, G.S. Ansell, Trans. ASM. 60 (1967) 242.
- [9] R.B. Benson, R.K. Dann, L.W. Roberts, Trans. AIME. 242 (1968) 2199.
- [10] R.M. Vennett, G.S. Ansell, Trans. ASM. 62 (1969) 1007.
- [11] R.J. Walter, R.P. Jewitt, W.T. Chandler, Mat. Sci. Eng. 5 (1969) 98.
- [12] M.R. Louthan, G.R. Caskey, J.A. Donovan, D.E. Rawl, Mat. Sci. Eng. 10 (1972) 357.
- [13] A.W. Thompson, Ductility Losses in Austenitic Stainless Steels Caused by Hydrogen, Hydrogen in Metals, ed. I.M. Bernstein, A.W. Thompson, ASM, Cleveland, 1974, p. 91.
- [14] D.A. Vaughn, D.I. Phalen, C.L. Peterson, W.K. Boyd, Corros. 19 (1963) 315t.
- [15] D.L. Douglass, G. Thomas, W.R. Roser, Corros. 20 (1964) 15t.
- [16] P.J. Greeley, V.J. Russo, R.K. Saxer, J.R. Myers, Corros. 21 (1965) 327.
- [17] M.L. Holzworth, M.R. Louthan, Corros. 24 (1968) 110.

- [18] H.K. Birnbaum, C.A. Wert, Ber. Bunsen Ges. 76 (2002) 806.
- [19] S.S. Birley, D. Tromans D, Corros. 27 (1991) 63.
- [20] M.B. Whiteman, A.R. Shamakian, Corros. 21 (2005) 53.
- [21] R. Lagneborg, J. Iron. Steel. Inst. 207 (1999) 363.
- [22] M.L. Holzworth, Corros. 25 (2001) 107.
- [23] L.K. Zamiryakin, Sov. Mater. Sci. 7 (2004) 9.
- [24] R.M. Vennet, G.S. Ansell, Trans. ASM. 60 (2003) 242.
- [25] R.B. Benson, R.K. Dann, L.W. Robert, Trans. AIME. 242 (1999) 2199.